2022 44th Annual International Conference of
the IEEE Engineering in Medicine & Biology Society (EMBC)
Scottish Event Campus, Glasgow, UK, July 11-15, 2022

2022 44th Annual International Conference of the IEEE Engineering in Medicine & Biology Society (EMBC) | 978-1-7281-2782-8/22/$31.00 ©2022 IEEE | DOI: 10.1109/EMBC48229.2022.9871874

A Wireless System for EEG Acquisition and Processing in an Earbud Form Factor with 600 Hours Battery Lifetime

Marco Guermandi[1], Andrea Cossettini[2], Simone Benatti[3,1] and Luca Benini[2,1]

***Abstract*— In recent years, in-ear electroencephalography (EEG) was demonstrated to record signals of similar quality compared to standard scalp-based EEG, and clinical applications of objective hearing threshold estimations have been reported. Existing devices, however, still lack important features. In fact, most of the available solutions are based on wet electrodes, require to be connected to external acquisition platforms, or do not offer on-board processing capabilities. Here we overcome all these limitations, presenting an ear-EEG system based on dry electrodes that includes all the acquisition, processing, and connectivity electronics directly in the ear bud. The earpiece is equipped with an ultra-low power analog front-end for analog-to-digital conversion, a low-power MEMS microphone, a low-power inertial measurement unit, and an ARM Cortex-M4 based microcontroller enabling on-board processing and Bluetooth Low Energy connectivity. The system can stream raw EEG data or perform data processing directly in-ear. We test the device by analysing its capability to detect brain response to external auditory stimuli, achieving 4 and 1.3 mW power consumption for data streaming or on board processing, respectively. The latter allows for 600 hours operation on a PR44 zinc-air battery. To the best of our knowledge, this is the first wireless and fully self-contained ear-EEG system performing on-board processing, all embedded in a single earbud.**

***Clinical relevance*— The proposed ear-EEG system can be employed for diagnostic tasks such as objective hearing threshold estimations, outside of clinical settings, thereby enabling it as a point-of-care solution. The long battery lifetime is also suitable for a continuous monitoring scenario.**

I. INTRODUCTION

Electroencephalography (EEG) is a commonly used clinical tool to analyze brain activity. Applications of EEG span from the development of brain-computer interfaces (BCI), to the monitoring and detection of severe neural diseases, such as epilepsy or Autism Spectrum Disorders (ASD). The golden standard is represented by scalp-EEG systems, consisting of caps equipped with multiple electrodes positioned on the scalp. However, the need for long wires to connect electrodes to a recording module enhances interference and motion artifacts [1]. At the same time, these systems are cumbersome and make the users uncomfortable because of perceived stigmatization, motivating major research efforts towards wearable solutions [2].

Several groups are working on the development of small EEG systems that can be placed behind-the-ear or even in-ear (ear-EEG). These approaches have been demonstrated capable of capturing signals closely related to the scalp-EEG ones [3], [4], [5]. While a fundamental limitation of ear-EEG is its spatial resolution, the high correlation of EEG signals between one location and its surroundings allows ear-EEG to record information not only from the temporal lobes but also from the frontal, occipital, parietal and central ones [6]. These results demonstrate that ear-EEG is a viable approach for future unobtrusive EEG systems.

A major challenge for ear-EEG is the selection of the electrodes. In general, EEG electrodes can be classified in two main categories: wet and dry. While wet solutions guarantee better electrode-skin impedance, gel tends to dry over time, thereby progressively reducing signal quality [7], [8]. Consequently, to guarantee stable performance and minimize human intervention and discomfort, dry electrode solutions are preferred. Various designs of dry-contact electrodes have been proposed, including mesh electrodes laminated onto the skin [9], flexible polymer based electrodes [10], [11], [12], and spring-loaded electrodes [13], [14]. Among these, taking into account the noise figure, sintered silver-silver chloride (Ag/AgCl) and Ag/AgCl plating on silver proved to offer the best low-noise performance for EEG [15]. Such dry solutions, however, need to be properly coupled to the acquisition electronics.

The second challenge for ear-EEG is set by the readout electronics, which should be concealed (possibly, entirely in the ear), low power (for sufficient battery duration), and equipped with on-board computation capabilities (to perform processing on-the-edge, avoid the need of a companion device and continuous data transmission to such device).

The first ear-EEG solution was proposed in [16], where authors developed personalized earpieces and successfully recorded alpha waves. However, the fabrication process was complex and costly, and the materials used were hard, which can bring discomfort for long-term wear. Building up from these results, a number of other systems have been proposed, successfully recording alpha waves, acoustic steady state response (ASSR), and auditory or visual evoked potentials.

Simpler customized earpieces have been proposed in [17], but they required conductive gels and external amplifiers

This work was supported by the Swiss National Science Foundation (Project PEDESITE) under grant agreement 193813.

[1]Department of Electrical, Electronic and Information Engineering "Guglielmo Marconi" (DEI), University of Bologna, Bologna, Italy marco.guermandi, simone.benatti, luca.benini@unibo.it

[2]Department of Information Technology and Electrical Engineering, ETH Zürich, Zürich, Switzerland cossettini.andrea@iis.ee.ethz.ch, lbenini@iis.ee.ethz.ch

[3]Dipartimento di Ingegneria "Enzo Ferrari" (DIEF), University of Modena and Reggio Emilia, Modena, Italy simone.benatti@unimore.it

All the experimental procedures presented in this paper followed the principles outlined in the Helsinki Declaration of 1975, as revised in 2000.

(g.USBamp, by g.tec). Attempts to move towards generic earpieces include systems like[18][19]; however, they required conductive gels or had low durability with enhanced low-frequency noise. A more advanced system has been presented by[10]: in-ear headphones, with buds based on carbon nanotubes CNT/PDMS loaded on silicone substrate, capable of triggering sound stimulations while recording EEG signals. However, they relied on materials difficult to produce, and also needed an external acquisition system (BIOPAC) for signal recording.

A personalized design that perfectly fits the ear also capable of in-ear signal conditioning in a miniaturized form factor is presented by [20], with an 8 mm^2 chip in 65-nm CMOS with on-board amplification, an integrated Body Area Network transceiver, and total power consumption of 82.9 µW. However, despite the impressively low power consumption, such solution still does not provide on-board processing capabilities. In [21], instead, 6 dry electrodes are included in the ear, and they are connected to a small printed circuit board (PCB) of 25×25 mm^2 that provides neuro-modulation, data aggregation on a Microsemi SmartFusion2 field-programmable gate array (FPGA), and Bluetooth Low Energy (BLE) connectivity. However, despite the availability of computational resources on the FPGA, the processing done is minimal; furthermore, the PCB and the battery are not integrated directly in-ear.

In summary, none of the existing solutions can satisfy all the key design requirements for truly unobtrusive, concealed, low-power, processing-capable, all-in-ear systems. Nevertheless, despite the current system design limitations, a number of different applications have been empowered by ear-EEG, including objective hearing threshold estimations [22]. A fully in-ear system with processing capabilities would enable to take such applications to the next level, e.g. offering hearing threshold estimations as point-of-care (PoC) solutions and furthermore enabling a host of continuous monitoring applications..

Within this framework, this paper presents an ear-EEG system solution based on dry electrodes, equipped with ultra-low power analog front-end (AFE) acquisition electronics, ARM Cortex-M4 based computation capabilities, and BLE connectivity, all embedded in a single earbud (15×16 mm^2 PCB). The system is capable of streaming raw EEG data or performing on-board processing to transmit only the results of computation at only 1.3 mW, allowing more than 600 hours of operation on a PR44 zinc-air battery. We show how the system is capable of acquiring the EEG signal to extract the response from an auditory stimulus and process it in order to detect the presence or absence of such a response. This demonstrates the potential of the system to be used for diagnostic tasks, such as objective hearing threshold estimation outside of clinical settings.

II. SYSTEM DESCRIPTION

A. In-Ear EEG Acquisition System

The system is depicted in Fig. 1. It supports the acquisition of up to 3 differential channels (of which 2 simultaneously),

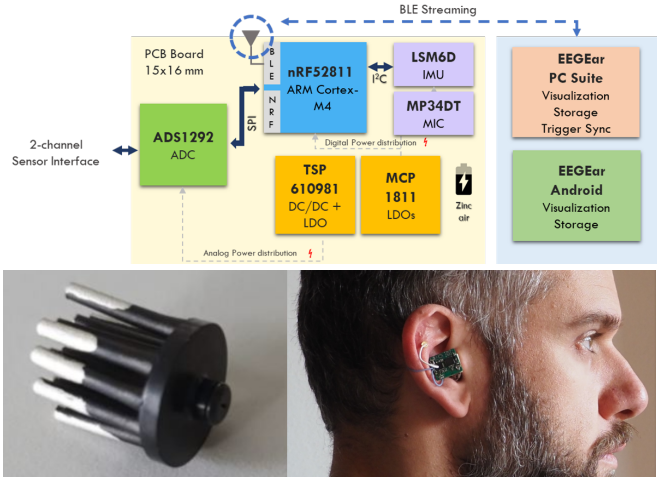

Fig. 1. Top: Scheme of the full system. Bottom: photo of the in-ear electrode and of the system worn by a subject.

although the interface with the skin is obtained through two different types of dry electrodes. In the ear canal, we adopted a custom electrode fabricated by Dätwyler Holding Inc. [23], derived from their SoftPulse dry electrodes family. The bulk of the device is composed of a conductive elastomer, while the area in contact with the skin is covered with silver/silver-chloride to optimize the electrical interface. In this prototype, signal amplification stages can be connected to the electrode through a standard snap connector. With respect to commercial electrodes of the SoftPulse family, the ones used in this prototype are characterized by longer posts and, since contact with the skin is obtained on the walls of the posts rather than on the tips, the silver/silver chloride coating extends for approximately 5 mm from the tip.

The reference and bias electrodes are 4 mm diameter neodymium magnets coated in gold. This allows flexible placing virtually anywhere in the ear, with very good mechanical stability without the need for custom earpieces. In the framework of this paper, reference and bias electrodes are placed respectively on the outer and inner sides of the ear scapha.

The electronics for signal conditioning, processing and data transmission is hosted on a 15x16 mm^2 PCB. The sensing part comprises an AFE for analog-to-digital conversion (ADS1292, from Texas Instruments), a low power MEMS microphone (MP34DT05TR-A, from STMicrolectronics), a low-power Intertial Measurement Unit (IMU, LSM6DSLTR, from STMicroelectronics) with a 3D accelerometer, 3D gyroscope and integrated temperature sensor. The AFE is in the same product family of the ADS1298, which has been proved to be able to acquire EEG signals without significantly degrading noise performance with respect to products specifically targeting EEG signal acquisition, such as ADS1299 [24].

The system is powered by a low-cost, high energy density 1.4 V PR44 zinc-air disc battery, typically used in hearing aids. The weight is only 1.9 grams, with a 11.5 mm di-

ameter and 5 mm height. The rated capacity is 610 mAh. A high-efficiency boost converter (TPS610981, from Texas Instruments) steps up the system power supply to 3.3V. This is used for the analog supply of the AFE and to feed to two Low DropOut Linear regulators (LDOs) providing the 1.8V digital supplies of the AFE and microcontroller unit (MCU), and supply to the remaining sensors.

Data acquisition and processing from the sensors is handled by a nRF52811 System-on-Chip (SoC) from Nordic Semiconductors, which also provides data communication capability. The ARM Cortex-M4 MCU running at 64 MHz allows flexible Bluetooth 5.1 (BLE) communication at a low-power budget, and Bluetooth direction-finding capabilities. For a 1 Mbps link, the power consumption of the radio is 13.8 mW when transmitting data at 0 dBm output power, and 15.6 mW when receiving data. The power consumption can be reduced down to 3.6 μW with system ON, full RAM retention, and 1 μW with system OFF. A 14x5.0x0.1 mm^3 FXP840 flexible antenna from Taoglas is used for BLE TX/RX. Its small size and flexibility make it ideal for size-constrained applications.

The system can operate in four modalities:

- **Advertising Mode.** Ultra low power mode. The acquisition is stopped, and the MCU and the BLE radio are OFF, but wake up periodically to detect if a device is ready to connect via BLE.
- **Connected Mode.** Low power mode. The acquisition is stopped, and the MCU and BLE radio periodically wake up to keep the connection open.
- **Streaming Mode.** The acquisition is running at 500 SPS, and data is acquired, converted to digital, and streamed to the host device.
- **On Board Computing Mode.** The acquisition is running at a programmable data rate, and data is acquired, converted to digital, and streamed to the host device. BLE is connected, and the radio is only used for synchronization data (triggers) from the host to the device and for sending the results of computation from the device to the host (i.e., when a response to the stimulus is detected).

B. Data transmission and trigger management

In streaming mode, data is sent in 242 byte packets containing a 1 byte header, a 1 byte footer and 30 data sub-packets. Each of them contains one 24-bit sample per channel and 2 additional bytes to store additional information. One of these is generally used to store synchronization information (triggers). To maximize the synchronization quality, the trigger signal (represented by 1 byte, allowing 256 different trigger levels), is sent via BLE from the device presenting the stimulus (e.g., a Personal Computer) to the ear-EEG device. Received triggers are appended to the current sub-packet. Once the whole packet is filled and ready, it is transmitted back to the PC, including the trigger information, synchronized to the correct samples from the AFE. In this way, the maximum uncertainty in the trigger instant is limited to the length of a minimum connection interval which is below 8 ms.

Due to its very low amplitude, the EEG signal is particularly prone to suffer a quality degradation from any type of external noise or interference coupling to the signal itself. BLE transmission can lead to this kind of issue for two reasons: electromagnetic interference from the signal radiating from the antenna and supply noise due to the significant peak currents in the order of tens of mA that are drawn by the RF transceiver when transmitting or receiving data. This is exacerbated by the reduced size of the device, which puts noisy digital and RF sections in close proximity to the sensitive electrodes and AFE. While this is hardly a concern for regular EEG, it can become a problem for ear-EEG, where signals have very small amplitude, especially when dealing with evoked potentials. As described above, a trigger signal needs to be sent to the device every time a stimulus is presented to the subject. If the trigger is sent simultaneously to the stimulus presentation, a situation like the one presented in Fig. 2 can occur. In this case, 500 epochs of in-ear EEG signal are averaged in order to reduce uncorrelated noise (endogenous background noise and electrical noise). Since the start of the epoch is marked by a trigger signal sent to the device, it will always occur at the same time and averaging will not reduce its amplitude. Fig. 2 clearly shows not only a peak around 10 ms but also repetitive peaks every approximately 60 ms (TX interval for 500 SPS streaming).

In order to avoid this effect, each trigger signal is delayed by a random amount of time (from 0 to 100 ms). The trigger data sent to the device contains information on the delay, which is appended to the samples. The exact time at which the epoch starts can then easily be computed, either on the device itself for online processing or on the remote PC when in streaming mode. In this way, interference from the BLE transceiver becomes uncorrelated noise and gets averaged out when reconstructing the evoked potential.

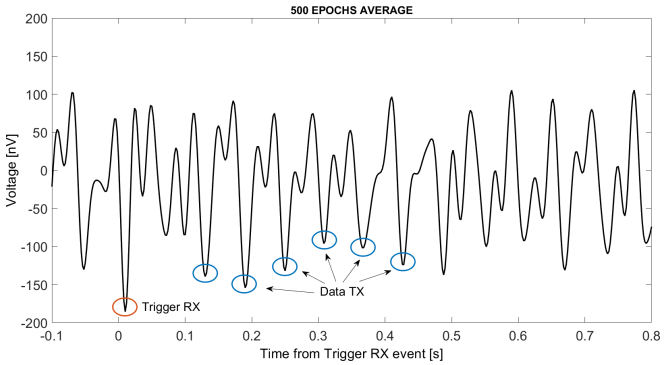

Fig. 2. When the trigger is synchronized with the stimulus, noise due to BLE TX/RX becomes correlated to the stimulus and the evoked potential response. The noise amplitude can be comparable with that of the evoked potential and, since correlated, does not get averaged out. When the device is in streaming mode, noise looks periodic with a period equal to that of the TX interval (60 ms for 500 SPS data rate).

C. Stimulus Selection and On-board Signal Processing

In this work we want to demonstrate how the developed system can reliably detect a brain response evoked by auditory stimuli, performing signal acquisition and processing in a system completely enclosed in an earbud-like form factor. For this purpose, we want to adopt an experimental setup that enables a good trade-off between algorithm complexity and sensitivity.

Auditory stimulus analysis, as for every potential evoked by an external stimulus, can be split in two large classes, depending on whether analysis is performed in the time domain (proper auditory evoked potentials or AEP) or in the frequency domain (Auditory Steady State Response, ASSR). The analysis of the latter obviously requires an additional step of conversion of the signal from the time to the frequency domain. For example, systems for hearing threshold estimation from ASSR commonly involve either a Fourier Transform or an adaptive filtering algorithm called the Fourier Linear Combiner, followed by F-test statistical analysis [25]. While the significant computational burden introduced by the analysis algorithm is negligible when analysis is performed off-line or on a personal computer, it becomes of major importance when the analysis is moved to a wearable EEG acquisition system with extremely limited available energy, as in our case.

Fig. 3 presents the average of 500 responses of a test subject to a White Gaussian Noise stimulus, lasting 50 ms, as detected by the system. The Inter Stimulus Interval (ISI) is 500 ms plus a random jitter comprised between 0 and 200 ms. The random jitter is added to increase the amplitude of the response, as typically done in evoked potential setups [26]. The low-frequency portion of the signal is generally characterized by a very low signal to noise ratio (SNR) and interference from the mains at 50/60 Hz and its harmonics can easily be orders of magnitude higher than the signal itself, as typical for dry electrode systems with no skin preparation and quick setup [27]. For this reason, the signal is band pass filtered between 8 and 48 Hz. The noise level is normally in the range of 200 to 400 nV peak-to-peak, whereas the peak response is between 300 and 500 nV, depending on subject and contact quality.

Fig. 4 presents the response to a stimulus sequence similar to the one in Fig. 3, except that, in this case, each stimulus is comprised of a sequence of three 50 ms white Gaussian noise pulses, separated by 50 ms of silence. It is quite clear how, despite the large number of averaged epochs, the response to the second and third pulses is below noise level, making the presentation of periodic, closely-spaced sound pulses quite ineffective in eliciting a proper response. If on one side this effect has been already observed in literature in standard EEG setups, one should notice how the very low SNR that can be obtained from an in-ear setup aggravates the effect.

Given the fact that the system is clearly able to detect an evoked potential response in the time-domain and the need to limit the amount of processing to guarantee real-time analysis and to minimize the system power budget, we chose to adopt

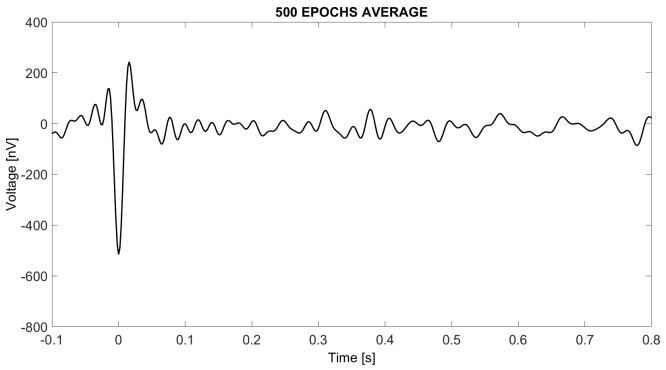

Fig. 3. In-ear EEG response evoked by a 50 ms white Gaussian noise stimulus. Average of 500 epochs. The origin of the x-axis is centered on the peak of the response.

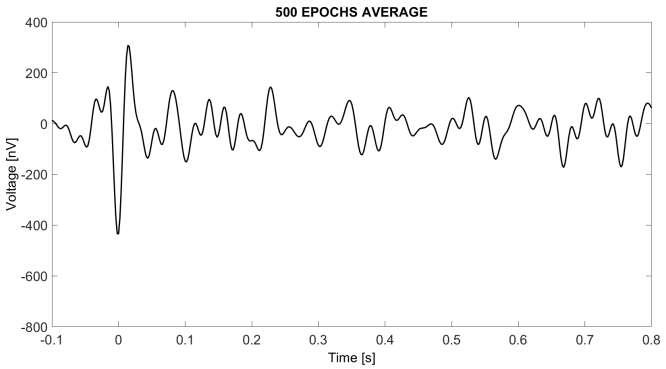

Fig. 4. In-ear EEG response evoked by a sequence of 50 ms white Gaussian pulses, separated by 50 ms of silence. When presented with a sequence of short separated stimuli with no random jitter in the ISI, the response to stimuli after the first gets below the noise level even after averaging over 500 epochs. The origin of the x-axis is centered on the peak of the response.

a paradigm based on the repetition of short sound pulses with an ISI characterized by a random duration, so as to maximize the response.

The signal is first filtered at run time, with a cascade of a band-pass filter (BPF) with 8 and 48 Hz cut-off frequencies, and an additional 50 Hz notch filter to increase rejection to 50 Hz noise from the mains. Normally, evoked responses are filtered with Finite Impulse Response (FIR) filters in order to avoid introducing phase non-linearities typical of Infinite Impulse Response (IIR) filters. Since the price to pay is a significant increase in the computational complexity of the filters, we chose to use 8th order Blackmann IIR filters for both the BPF and notch filters.

The response to the stimulus is then windowed on a rectangular window centered on the peak response, as shown in Fig. 3. The epochs in which the signal exceeds the ± 8 μV range are removed to perform a simple artifact rejection. The windows related to the response to several stimuli are averaged, and the average is compared to a template response by computing the time-domain correlation of the two. A response to the stimulus is detected when the correlation is above a certain threshold.

In the following section, we analyze the performance of the system and of the algorithm for variable average ISI,

correlation window size and threshold. We also show how replacing FIR filters with IIR filters does not significantly affect the performance of the algorithm.

III. EXPERIMENTAL RESULTS

A. Electrical Characterization

The system supports data-rates from 125 SPS to 8 kSPS. In streaming mode, the system sampling frequency is limited to 500 SPS by the maximum average current that can be safely drawn from the battery without affecting its duration (approximately 8 mA). In the following, the sampling frequency will always be set to 500 SPS, which guarantees a -3dB bandwidth of 131 Hz, way above the standard EEG band upper frequency. Electrical characterization is also performed at this sample rate.

The system noise is measured by shorting the inputs of the AFE and integrating over the standard EEG band (0.5 to 100 Hz). Its value ranges between a maximum of 1.75 μV_{RMS} with a programmable gain amplifier (PGA) gain equal to 1 and a minimum of 0.47 μV_{RMS} with PGA gain equal to 12. Since the electrodes are characterized by different materials and interfaces, a constant DC bias offset appears at the AFE input. We chose not to remove it with an analog high pass filter to avoid introducing unnecessary bandwidth limitations. As a consequence, the maximum PGA gain that can be used is 8, characterized by a 0.49 μV_{RMS} noise. The Common Mode Rejection Ratio is measured at 110 dB. Both these values are in line with IFCN standards for the clinical recording of EEG signals [28].

B. Experimental Setup

Three healthy subjects with normal hearing took part in the experiments. The auditory stimuli (50 ms duration, white Gaussian noise) are presented from the speaker of a laptop running Psychtoolbox 3.0.18 for Windows in MATLAB R2020. Most of the following analysis is performed off-line, with data streamed to the same laptop and processed at a later stage. We also demonstrate on a few test cases how online embedded processing yields comparable results. A two-electrode differential setup is used, with one electrode in the ear channel while the reference and bias electrodes are placed on the scapha of the same ear. The setup is therefore fully enclosed in the ear of the subject. Triggers generated by the stimulation program were bound to the incoming raw data by a custom software, as described in the previous section. A first training session of 5 minutes is used to build a template for the response of each subject. This is obtained from averaging 500 epochs, with stimuli presented at an average ISI of 600 ms. A 5 minute resting state session is also acquired with the same setup with speakers turned off, to be used as control for specificity characterization. In the following, we analyze the performance of the system in recognising whether the subject is hearing or not the presented stimulus. The performance is presented for varying parameters of the algorithm (correlation threshold TH, correlation window size CWS, and number of epochs N_{epochs}) and of the stimulus (average ISI).

For each of the 5 tested ISI, we acquire the response to 1000 stimuli (active session), requiring approximately a 30 minute recording session. In order to randomize results further without increasing the already significant experimental time, for each subject we build 1000 random permutations of the epoch order. The first N_{epochs} per each permutation are averaged, and a window of CWS samples around the peak response is correlated to the template. If the correlation is above threshold TH, the algorithm output is TRUE,

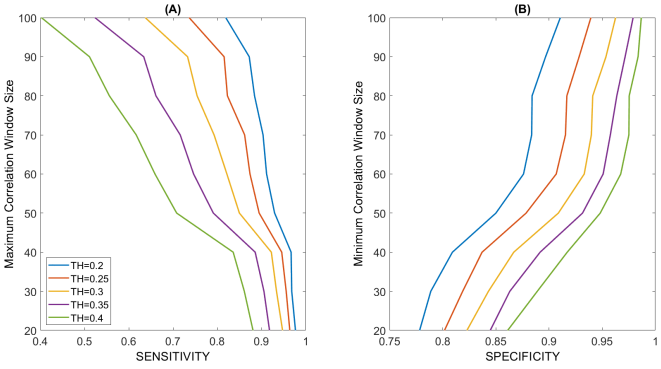

Fig. 5. Correlation window size (in number of samples), necessary for achieving a certain sensitivity (A) and specificity (B) in recognising if the stimulus is perceived by the subject. Data for average of 100 epochs, 0.6 s average ISI, variable threshold between 0.2 and 0.4.

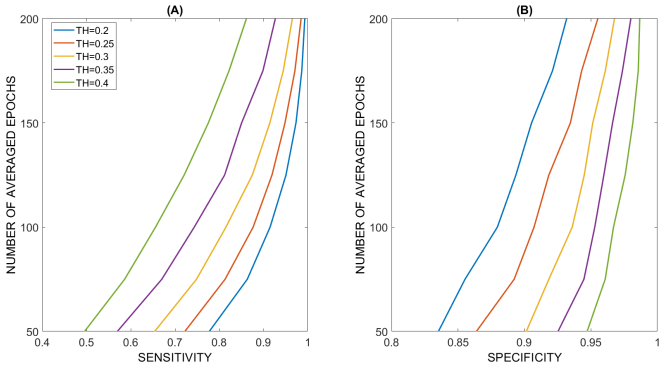

Fig. 6. Number of epochs necessary to achieve a certain sensitivity (A) and specificity (B). Data for 0.6 s average ISI, variable threshold between 0.2 and 0.4.

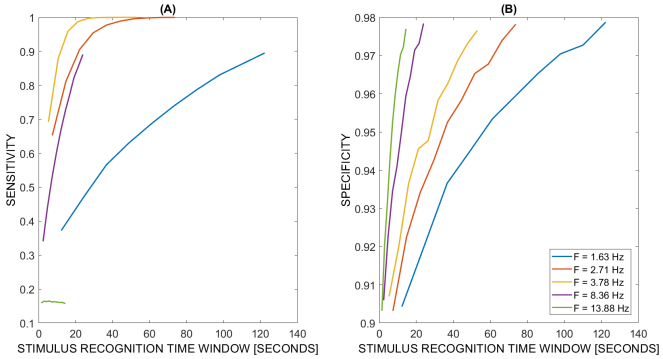

Fig. 7. Minimum time necessary to achieve a certain specificity and sensitivity, as a function of the average ISI.

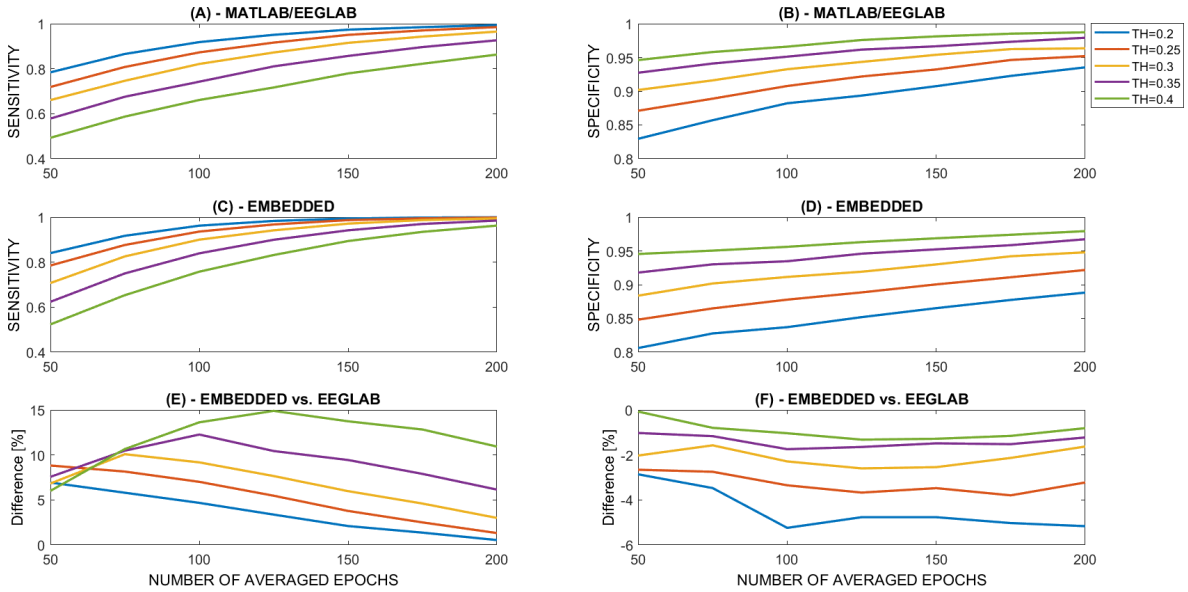

Fig. 8. Comparison of sensitivity and specificity achieved with embedded processing vs. MATLAB/EEGLAB offline processing.

predicting the subject is hearing the stimulus. This is done for both the active and resting state sessions.

Sensitivity and specificity are then computed as:

$$Sensitivity = N_{TRUE,active}/1000 \tag{1}$$

$$Specificity = 1 - (N_{TRUE,resting}/1000) \tag{2}$$

where $N_{TRUE,active}$ and $N_{TRUE,resting}$ are the number of TRUE outputs on the active and resting state sessions respectively.

Data for the three subjects are then averaged to provide the final plots.

C. Analysis of Results

Fig. 5 presents the results in terms of correlation window size (in samples) needed to achieve specific levels of sensitivity and specificity. The correlation threshold is variable between 0.2 and 0.4, and the average ISI is 600 ms. Due to random noise and the signal power decreasing at increasing distance from the peak, a larger window size reduces the correlation and therefore the likelihood of the algorithm returning a TRUE. For this reason and from eqs. III-B and III-B, for sensitivity, it is plotted as a maximum value, for specificity as a minimum value. Of course, a larger CWS also increases the computational burden.

Fig.6 shows the minimum number of epochs needed to achieve a certain value of specificity and sensitivity. The correlation threshold is variable between 0.2 and 0.4, the average ISI is 600 ms, and CWS is 60 samples. We can observe how a relatively small amount of epochs such as 50 is already enough to obtain both specificity and sensitivity above 80%, with a threshold of 0.2, while 90% can be achieved with as low as 120 epochs and a threshold of 0.25. A 95% sensitivity can finally be achieved with 170 epochs and a threshold of 0.3. Different values of the three parameters can be traded off to penalize sensitivity in favour of specificity and vice versa, depending on the application target confidence requirements.

The third performance parameter of primary importance for this type of system is the time required to recognize the presence or absence of the stimulus (see Fig. 7). This is essentially a function of the number of the averaged epochs (and therefore of the stimuli to be presented) and of the average frequency at which they are presented. In Fig. 7, we present data for 5 different average stimulus repetition rates comprised between 1.63 and 13.88 Hz. The threshold is fixed at 0.275 and CWS to 60 samples. We can observe how the maximum speed for a given sensitivity is achieved around 4 stimuli per second, since below that repetition frequency the accuracy is not significantly influenced by the ISI. For higher repetition frequencies, the performance starts to drop until reaching a negligible value of sensitivity above 10 Hz. As a reference, in a state-of-the-art ear-EEG system as [21], 100 s trials were needed to elicit an ASSR response with a relevant SNR and, in [22], a total stimulation time of 544 seconds was used to estimate the presence of a response for hearing threshold estimation. Although these results are not directly comparable, we can observe how the presented system promisingly compares with the performance of state-of-the-art systems, with the advantage of being fully integrated inside the user's ear.

Finally, Fig. 8 compares the results in terms of sensitivity and specificity achieved with the algorithm as implemented for embedded processing (with 8th order IIR filters, floating point, 32-bit precision) vs. MATLAB/EEGLAB offline processing (with 820 coefficient FIR filters). The different filter characteristics slightly improve sensitivity at the expense of specificity. Overall, the performance can be considered

similar. However, the computational burden is reduced by a factor 60x thanks to the replacement of FIR filters with IIR filters.

IV. CONCLUSIONS

In this paper, we presented an ear-EEG system based on dry electrodes, ultra-low power AFE, and ARM Cortex-M4 based MCU enabling on-board computation capabilities and BLE connectivity. The acquisition electronics is integrated into a small PCB of 15×16 mm^2, embedded into a small earbud form factor, and powered by a low-cost high-energy-density zinc-air battery. The system can operate in streaming mode, to transmit raw EEG data to a host device, or in on-board computing mode, transmitting to the host device only the results of on-board processing at only 1.3 mW, thereby enabling more than 600 hours of operation time. We demonstrated the performance of the system in detecting responses to auditory stimuli on three healthy subjects, proving that sensitivity and specificity levels above 80% can be achieved with a small number of epochs (50) and acquisition times are comparable to state-of-the-art. The proposed solution could be integrated into standard earbuds or hearing aid devices. To the best of our knowledge, this is the first ear-EEG system with on-board processing completely embedded in an earbud-like form factor with almost one month of battery lifetime, and these results demonstrate the potential of the system to be used for objective hearing threshold estimation outside of clinical settings.

REFERENCES

[1] W. O. Tatum, B. A. Dworetzky, and D. L. Schomer, "Artifact and recording concepts in eeg," *Journal of clinical neurophysiology*, vol. 28, no. 3, pp. 252–263, 2011.

[2] E. Bruno, P. F. Viana, M. R. Sperling, and M. P. Richardson, "Seizure detection at home: Do devices on the market match the needs of people living with epilepsy and their caregivers?" *Epilepsia*, vol. 61, pp. S11–S24, 2020.

[3] K. B. Mikkelsen, S. L. Kappel, D. P. Mandic, and P. Kidmose, "EEG recorded from the ear: characterizing the ear-EEG method," *Frontiers in neuroscience*, vol. 9, p. 438, 2015.

[4] M. G. Bleichner, B. Mirkovic, and S. Debener, "Identifying auditory attention with ear-EEG: cEEGrid versus high-density cap-EEG comparison," *Journal of neural engineering*, vol. 13, no. 6, p. 066004, 2016.

[5] I. Zibrandtsen, P. Kidmose, M. Otto, J. Ibsen, and T. Kjaer, "Case comparison of sleep features from ear-EEG and scalp-EEG," *Sleep Science*, vol. 9, no. 2, pp. 69–72, 2016.

[6] H. Dong, P. M. Matthews, and Y. Guo, "A new soft material based in-the-ear eeg recording technique," in *2016 38th Annual International Conference of the IEEE Engineering in Medicine and Biology Society (EMBC)*. IEEE, 2016, pp. 5709–5712.

[7] A. J. Casson, S. Smith, J. S. Duncan, and E. Rodriguez-Villegas, "Wearable eeg: what is it, why is it needed and what does it entail?" in *2008 30th Annual International Conference of the IEEE Engineering in Medicine and Biology Society*. IEEE, 2008, pp. 5867–5870.

[8] D. Looney, P. Kidmose, C. Park, M. Ungstrup, M. L. Rank, K. Rosenkranz, and D. P. Mandic, "The in-the-ear recording concept: User-centered and wearable brain monitoring," *IEEE pulse*, vol. 3, no. 6, pp. 32–42, 2012.

[9] J. J. Norton, D. S. Lee, J. W. Lee, W. Lee, O. Kwon, P. Won, S.-Y. Jung, H. Cheng, J.-W. Jeong, A. Akce *et al.*, "Soft, curved electrode systems capable of integration on the auricle as a persistent brain–computer interface," *Proceedings of the National Academy of Sciences*, vol. 112, no. 13, pp. 3920–3925, 2015.

[10] J. H. Lee, S. M. Lee, H. J. Byeon, J. S. Hong, K. S. Park, and S.-H. Lee, "Cnt/pdms-based canal-typed ear electrodes for inconspicuous eeg recording," *Journal of neural engineering*, vol. 11, no. 4, p. 046014, 2014.

[11] P. Fiedler, P. Pedrosa, S. Griebel, C. Fonseca, F. Vaz, E. Supriyanto, F. Zanow, and J. Haueisen, "Novel multipin electrode cap system for dry electroencephalography," *Brain topography*, vol. 28, no. 5, pp. 647–656, 2015.

[12] C.-T. Lin, L.-D. Liao, Y.-H. Liu, I.-J. Wang, B.-S. Lin, and J.-Y. Chang, "Novel dry polymer foam electrodes for long-term EEG measurement," *IEEE Transactions on Biomedical Engineering*, vol. 58, no. 5, pp. 1200–1207, 2010.

[13] P. Fiedler, S. Griebel, P. Pedrosa, C. Fonseca, F. Vaz, L. Zentner, F. Zanow, and J. Haueisen, "Multichannel EEG with novel Ti/TiN dry electrodes," *Sensors and Actuators A: Physical*, vol. 221, pp. 139–147, 2015.

[14] Y. M. Chi, Y.-T. Wang, Y. Wang, C. Maier, T.-P. Jung, and G. Cauwenberghs, "Dry and noncontact EEG sensors for mobile brain–computer interfaces," *IEEE Transactions on Neural Systems and Rehabilitation Engineering*, vol. 20, no. 2, pp. 228–235, 2011.

[15] P. Tallgren, S. Vanhatalo, K. Kaila, and J. Voipio, "Evaluation of commercially available electrodes and gels for recording of slow eeg potentials," *Clinical Neurophysiology*, vol. 116, no. 4, pp. 799–806, 2005.

[16] D. Looney, C. Park, P. Kidmose, M. L. Rank, M. Ungstrup, K. Rosenkranz, and D. P. Mandic, "An in-the-ear platform for recording electroencephalogram," in *2011 Annual International Conference of the IEEE Engineering in Medicine and Biology Society*. IEEE, 2011, pp. 6882–6885.

[17] P. Kidmose, D. Looney, and D. P. Mandic, "Auditory evoked responses from ear-eeg recordings," in *2012 Annual International Conference of the IEEE Engineering in Medicine and Biology Society*. IEEE, 2012, pp. 586–589.

[18] P. Kidmose, D. Looney, L. Jochumsen, and D. P. Mandic, "Ear-eeg from generic earpieces: A feasibility study," in *2013 35th annual international conference of the IEEE engineering in medicine and biology society (EMBC)*. IEEE, 2013, pp. 543–546.

[19] V. Goverdovsky, D. Looney, P. Kidmose, and D. P. Mandic, "In-ear eeg from viscoelastic generic earpieces: Robust and unobtrusive 24/7 monitoring," *IEEE Sensors Journal*, vol. 16, no. 1, pp. 271–277, 2015.

[20] J. Lee, K.-R. Lee, U. Ha, J.-H. Kim, K. Lee, S. Gweon, J. Jang, and H.-J. Yoo, "A 0.8-V 82.9-μW in-ear BCI controller IC with 8.8 PEF EEG instrumentation amplifier and wireless BAN transceiver," *IEEE Journal of Solid-State Circuits*, vol. 54, no. 4, pp. 1185–1195, 2019.

[21] R. Kaveh, J. Doong, A. Zhou, C. Schwendeman, K. Gopalan, F. L. Burghardt, A. C. Arias, M. M. Maharbiz, and R. Muller, "Wireless user-generic ear EEG," *IEEE Transactions on Biomedical Circuits and Systems*, vol. 14, no. 4, pp. 727–737, 2020.

[22] C. Bech Christensen, R. K. Hietkamp, J. M. Harte, T. Lunner, and P. Kidmose, "Toward eeg-assisted hearing aids: Objective threshold estimation based on ear-eeg in subjects with sensorineural hearing loss," *Trends in hearing*, vol. 22, p. 2331216518816203, 2018.

[23] "DATWYLER HOLDING Inc." https://datwyler.com/, 2022.

[24] M. Guermandi, S. Benatti, V. J. K. Morinigo, and L. Bertini, "A wearable device for minimally-invasive behind-the-ear eeg and evoked potentials," in *2018 IEEE Biomedical Circuits and Systems Conference (BioCAS)*. IEEE, 2018, pp. 1–4.

[25] K. R. Vander Werff, "Accuracy and time efficiency of two assr analysis methods using clinical test protocols," *Journal of the American Academy of Audiology*, vol. 20, no. 07, pp. 433–452, 2009.

[26] C. B. Christensen, J. M. Harte, T. Lunner, and P. Kidmose, "Ear-eeg-based objective hearing threshold estimation evaluated on normal hearing subjects," *IEEE Transactions on Biomedical Engineering*, vol. 65, no. 5, pp. 1026–1034, 2017.

[27] J. W. Kam, S. Griffin, A. Shen, S. Patel, H. Hinrichs, H.-J. Heinze, L. Y. Deouell, and R. T. Knight, "Systematic comparison between a wireless eeg system with dry electrodes and a wired eeg system with wet electrodes," *NeuroImage*, vol. 184, pp. 119–129, 2019.

[28] M. R. Nuwer, G. Comi, R. Emerson, A. Fuglsang-Frederiksen, J.-M. Guérit, H. Hinrichs, A. Ikeda, F. J. C. Luccas, and P. Rappelsburger, "Ifcn standards for digital recording of clinical eeg," *Electroencephalography and clinical Neurophysiology*, vol. 106, no. 3, pp. 259–261, 1998.